Supporting Information

Enhanced Isolation and Release of Circulating Tumor Cells using Nanoparticle Binding and Ligand Exchange in a Microfluidic Chip

Myoung-Hwan Park,[†,‡,∥,▼] Eduardo Reátegui,[⊥,#,△,▼] Wei Li,[†,§] Shannon N. Tessier,[⊥,#,△] Keith H. K. Wong,[⊥,#,△] Anne E. Jensen,[⊥] Vishal Thapar,[△] David Ting,[△] Mehmet Toner,[⊥,#] Shannon L. Stott,[*,⊥,△,¶] and Paula T. Hammond[*,†,‡,§]

[†]Department of Chemical Engineering, [‡]Institute for Soldier Nanotechnologies, and [§]David H. Koch Institute for Integrative Cancer Research, Massachusetts Institute of Technology, Cambridge, Massachusetts 02139, United States

[∥] Department of Chemistry, Sahmyook University, Seoul, 01795, Korea

[⊥]Center for Engineering in Medicine, [#]Department of Surgery, [△]Massachusetts General Hospital Cancer Center and [¶]Department of 10 Medicine, Massachusetts General Hospital, Harvard Medical School, Boston, Massachusetts 02114, United States

Synthesis of gold nanoparticles.

Gold nanoparticles (AuNPs) were prepared by following the Brust-Schiffrin two-phase method, using 1-pentanethiol as the capping ligand. To functionalize the NP surface, 30 mg of 1-pentanethiol protected gold nanoparticles (Au-C5) were mixed with 30 mg of COOH functionalized (MUA) and 90 mg of NHS ester functionalized (12-mercaptododecanoic acid NHS ester) thiol in 20 mL of dichloromethane (DCM). The solution was stirred in the dark for about 24 h, during which time the NPs precipitated out of solution. The precipitate in the reaction mixture was centrifuged and then washed twice with ether and DCM to remove free thiols. The resulting precipitate was dried in a vacuum and stored at 4 °C. Prior to use in the microfluidic device, the NPs were dissolved in methanol.

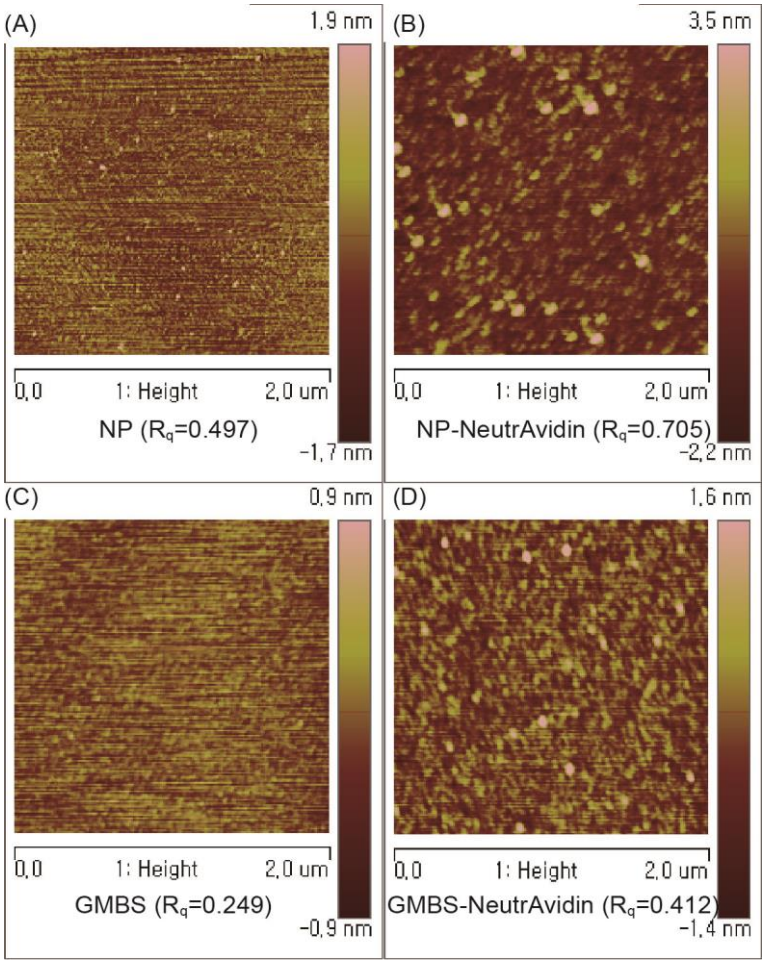

Figure S1. The topographic images of the NP-mediated chip substrates exhibit a corrugated surface generated by (a) the NP assemblies and (b) NP-NeutrAvidin binding, with R_q values of 0.497 nm and 0.705 nm, respectively. This is compared to (c) the GMBS and (d) GMBS-NeutrAvidin binding on smooth substrates with R_q values of 0.249 nm and 0.412 nm, respectively.

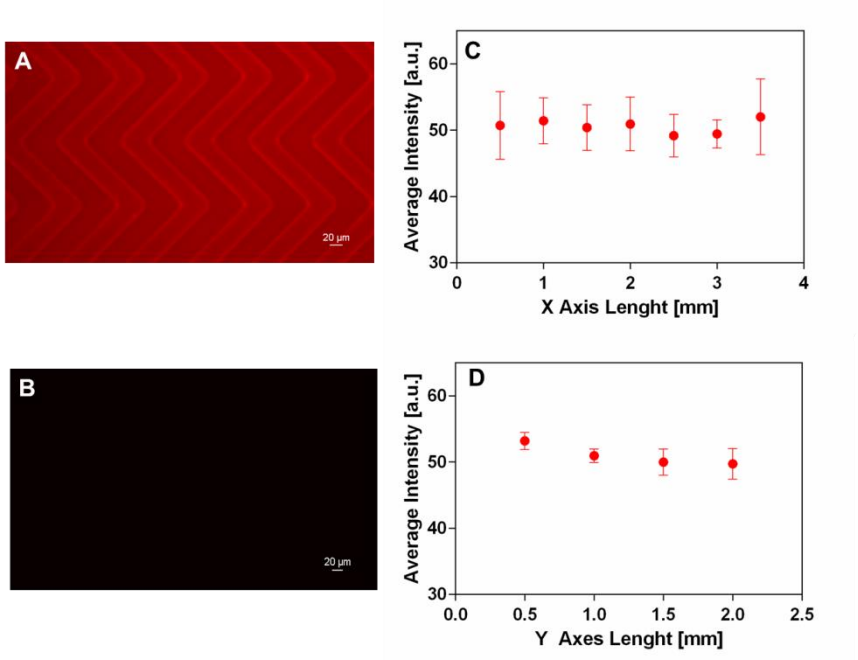

Figure S2. Fluorescence microscopy images of (A) a functionalized microfluidic surface with Biotin-RPE and (B) a control surface with a NP surface without neutravidin, demonstrating the deposition of NeutrAvidin on the surface of the microfluidic device. Quantification of the average fluorescence intensity along (C) the X axis and (D) the Y axis of the image shown in the Figure S2A. Five images per point were measured and three different devices were used.

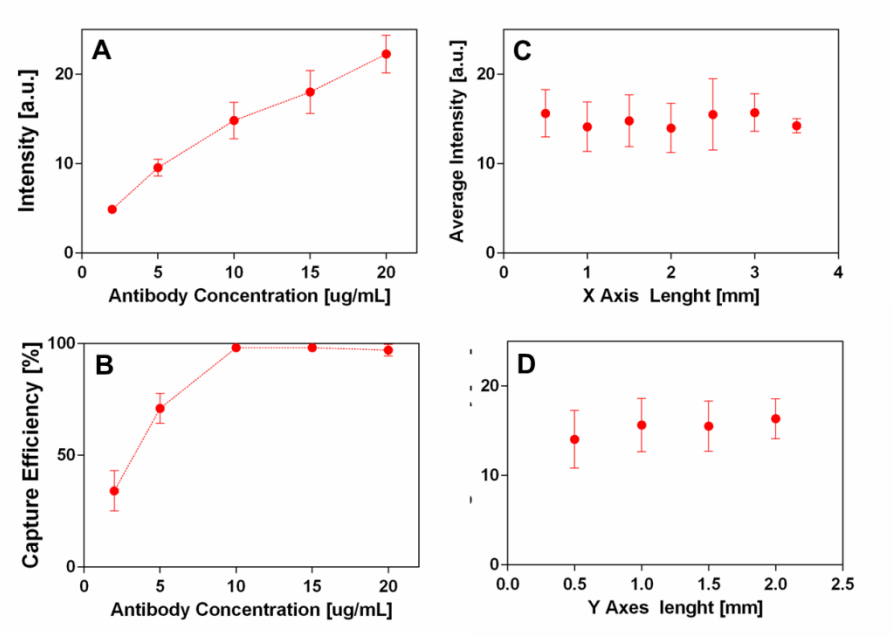

Figure S3. (A) Quantification of the amount of antibody on the surface with concentration used for immobilization onto a device and (B) capture efficiency of PC3 cells at different antibody concentrations. Quantification of the average fluorescence intensity along (C) the X axis and (D) the Y axis of the microfluidic device. For C & D a concentration of 10 ug/mL of a primary antibody was used and the secondary antibody was used according specifications of the manufacturer at 5 uL per 100uL of solution. Importantly, the correlated increase was observed in the capture efficiency of PC3 cells with the antibody coverage up to a concentration of 10 ug/mL, but the efficiency (98.15 ± 1.1 %) was saturated over than the antibody concentration (10 ug/mL) (Figure S3B). These results indicate that our experiments always with a use of an antibody concentration (>10 ug/mL) were performed in the high quality condition.

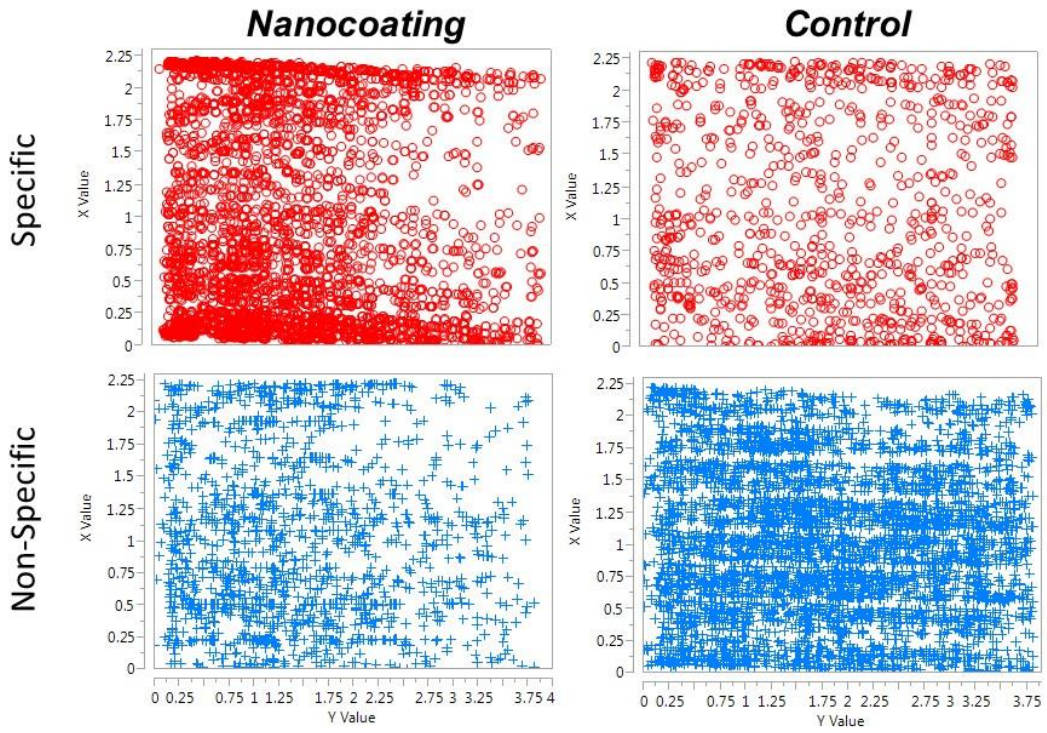

Figure S4. Heat map distribution of specific and non-specific cell capture of MDA-MB-231 CTCs on the surface of the microfluidic device.

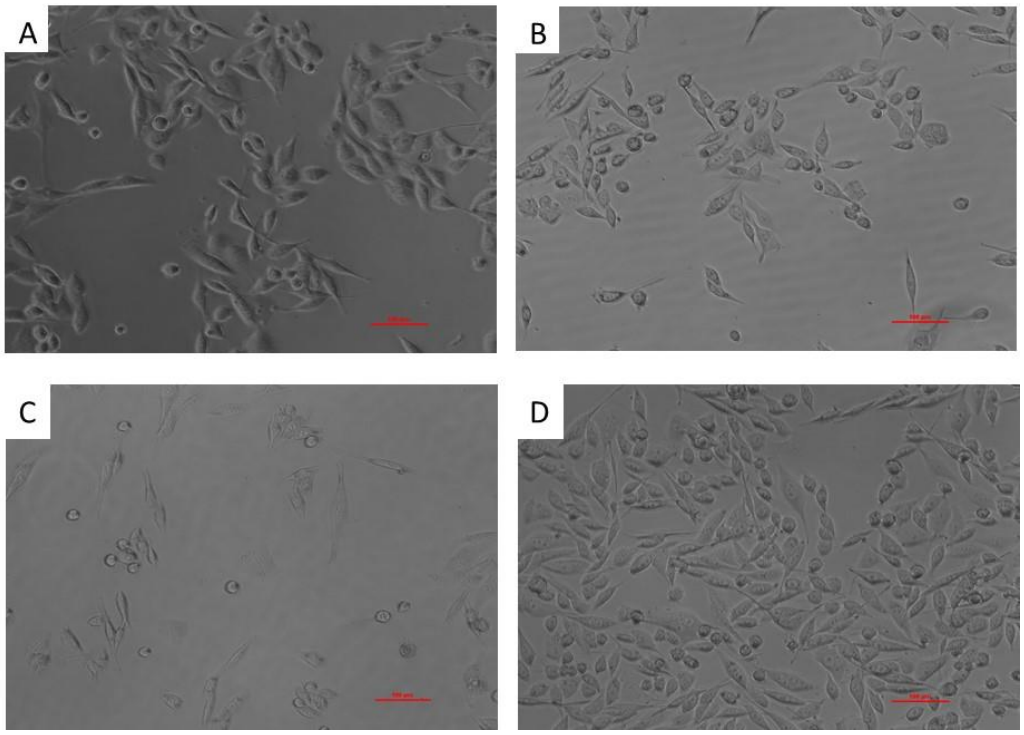

Figure S5. Cultured (A) PC3 and (B) MDA-MD-231 cells in the presence of GSH (1 mg/mL) for 4.5 h. Cultured cells (C) 1 day and (D) 5 days after GSH release from the nanocoating surface.

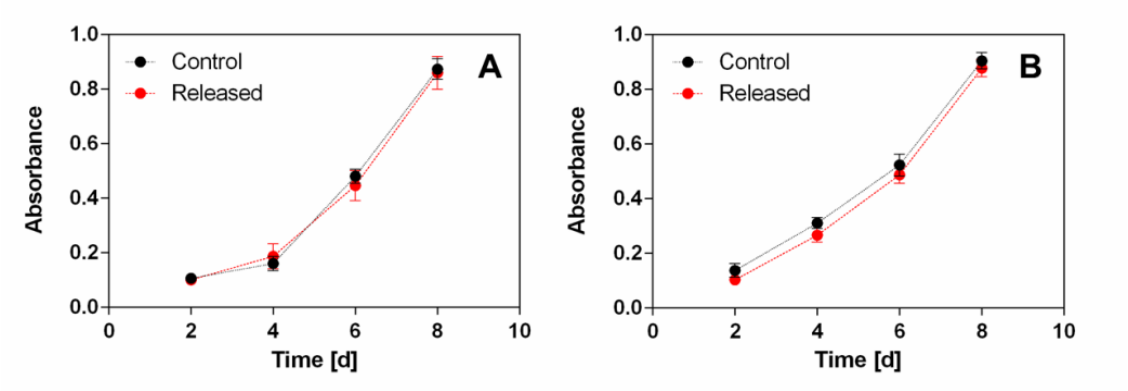

Figure S6. MTT assay performed with (A) the released PC3 and (B) the MDA-MB-231 cells by measuring the absorbance at 570 nm. Experiments were performed on triplicates and a control indicates untreated PC3 or MDA-MB-231 cells with our device. During 8 days, any significant difference in proliferation rate was not found for the control and released cells.

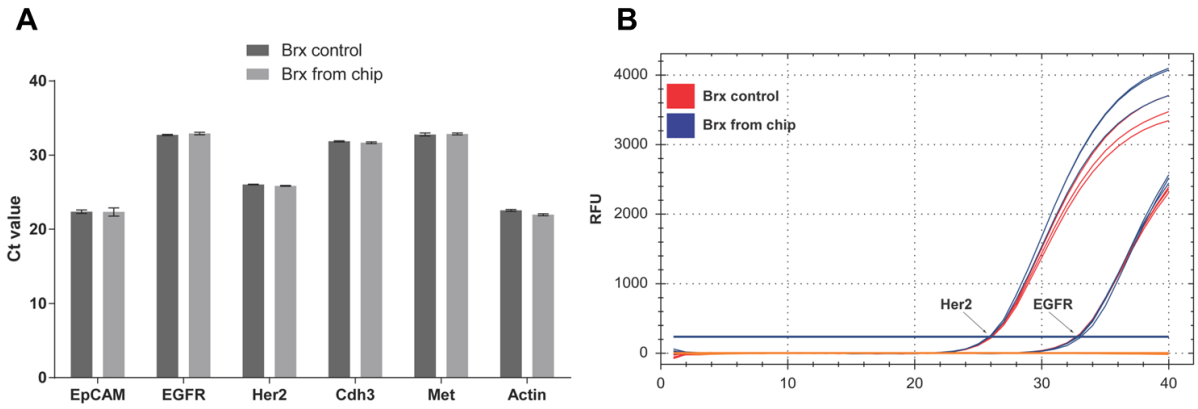

Figure S7. (A) Comparison of the Ct values for 6 genes obtained by RT-qPCR for control and released Brx cells. (B) Comparison of the amplification cycles for two of the genes used.

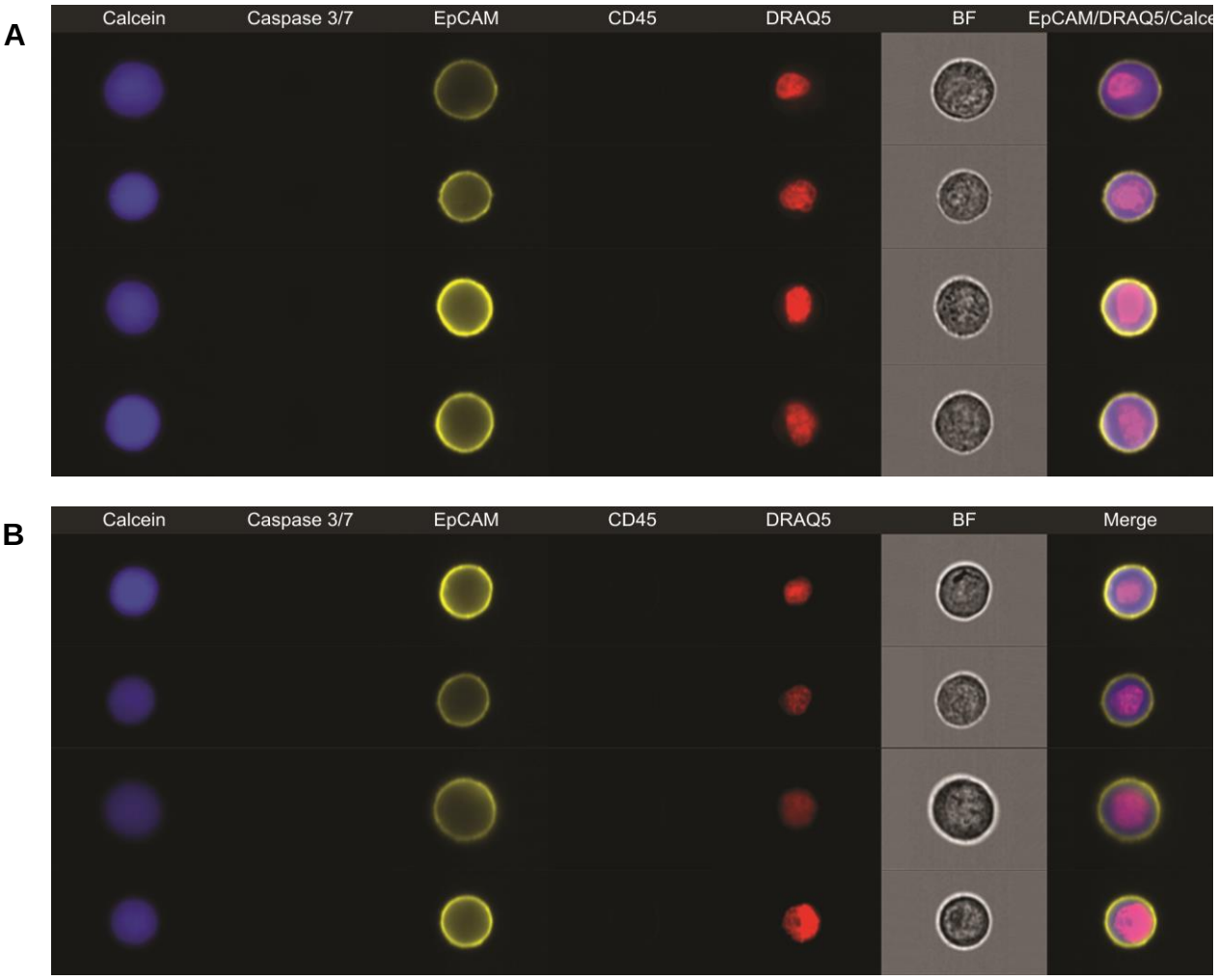

Figure S8. Imaging flow cytometry images of the two experimental groups: (A) Control Brx cells, and (B) Brx cells released from the microfluidic device.

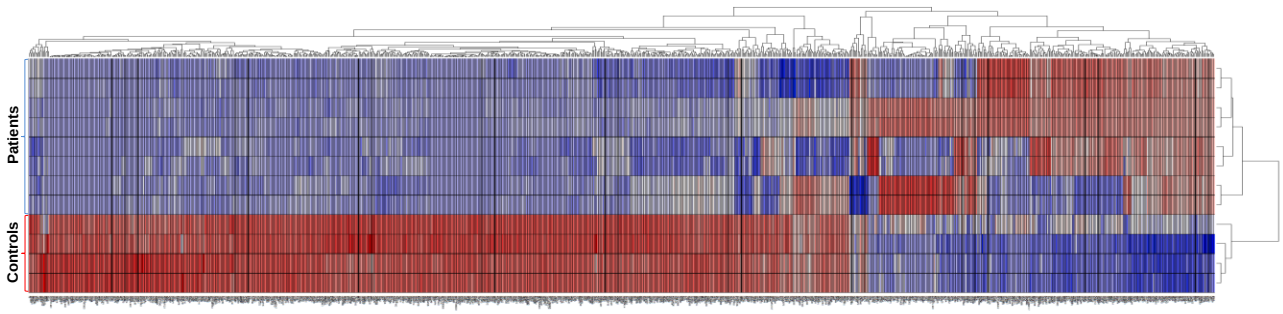

Figure S9. Unsupervised clustering of top 1000 most variant genes between breast patient samples and healthy controls. Each patient sample was analyzed as on-chip and release condition.

Table S1. Comparison of the Ct values of 5 genes across all samples.

	EpCAM		HER2		EGFR		CDH3		MET	
	Mean C_t	**S.D.**	**Mean C_t**	**S.D.**	**Mean C_t**	**S.D.**	**Mean C_t**	**S.D.**	**Mean C_t**	**S.D.**
PT1	27.70	0.12	27.54	0.11	ND		29.32	0.02	35.78	0.31
PT1R	27.97	0.14	27.84	0.04	ND		29.62	0.09	36.20	0.18
PT2	32.19	0.09	29.80	0.10	36.97	0.19	36.60	0.25	ND	ND
PT2R	30.39	0.11	28.22	0.09	35.61	0.23	35.07	0.37	ND	ND
PT3	33.68	1.25	30.76	0.11	28.81	0.18	36.44	0.45	31.53	0.12
PT3R	35.01	0.12	31.19	0.10	29.49	0.01	37.78	0.64	32.31	0.09
PT4	31.57	0.07	30.70	0.03	32.69	0.07	33.41	0.12	36.27	0.26
PT4R	29.42	0.19	28.64	0.10	30.96	0.03	31.22	0.15	33.64	0.08
H1	ND		ND		ND		ND		ND	
H2	ND		ND		ND		ND		ND	

Table S2. Set of 25 most variant genes between breast cancer patients and healthy controls

Gene	Description (Protein or RNA Level)	Ref. (#)
TFF1	Frequently expressed in breast tumors. Function in breast cancer is unknown.	1
AGR2	The human anterior gradient 2 (AGR2) is one of the targets of the estrogen receptor (ER), and it is an overexpressed gene in ER-positive breast cancer cell lines.	2
S100A16	Expression of this gene promotes epithelial to mesenchymal transition (EMT) via Notch1 pathway in breast cancer	3
KRT8	Expression of cytokeratin KRT8 differentiates distinct subtypes of grade 3 invasive ductal carcinoma of the breast.	4
KRT18	Expression of cytokeratin KRT18 differentiates distinct subtypes of grade 3 invasive ductal carcinoma of the breast.	4
MGP	Matrix Gia protein repression by miR-155 promotes oncogenic signals in breast cancer cell lines.	5
S100A14	Co expression with S100A16 correlates with a poor prognosis in human breast cancer and promotes cancer invasion.	6
CLCA2	Loss of this epithelial marker promotes EMT and indicates high risk of metastasis.	7
AZGP1	Decreased expression of AZGP1 is associated with poor prognosis on primary gastric cancer.	8
SCGB2A2	Expression of secretoglobin family 2A member 2 (SCGB2A2) has been detected in a high percentage of primary and metastatic breast tumors.	9
AGR3	Gene associated with the level of differentiation of breast cancer cells, slowly proliferation tumors, and more favorable prognosis of breast cancer.	10
FXYD3	Increased expression of the FXYD3 family of proteins has been associated with lung, colorectal cancer, and it also promotes cell proliferation in breast cancer as well.	11
TFF3	TFF3 protein expression is associated with larger tumor size, lymph node metastasis, higher stage, and poor survival outcome.	12
TM4SF1	Transmembrane 4 superfamily member 1(TM4SF1) is a member of tetraspanins group of proteins, it shows reduced apoptosis.	13
SERPIN3	Promotes endometrial cancer cell growth by regulating G2/M cell cycle checkpoint and apoptosis.	14
IFI27	At the protein level interferon alpha-inducible protein 27 (IFI27) promotes EMT transition and induces ovarian tumorigenicity and stemness.	15
CAV1	One of the genes involved in breast cancer progression.	16
SERPINE1	The serine protease inhibitor SERPINE1 is a poor prognosis biomarker in various cancers.	17
DKK1	Preferentially expressed in hormone-resistant breast tumors and in some common cancer types.	18
CD36	Mayor glycoprotein on the surface of platelets, it is involved in a variety of adhesive processes.	19
CD52	Present in a variety of lymphocytes, it is function in anti-adhesion in T-cells	20
PECAM1	Expressed in diverse cells of the vasculature, it has roles in angiogenesis, platelet function, thrombosis, and mechanosensing.	21
CXCR2	Key mediator in neutrophil migration.	22
BIN2	Involved in brain-neural function.	23
TRAC	Involve in the regulation of T-cell response.	24

References

(1) Prest, S. J.; May, F. E.; Westley, B. R. *FASEB J.* **2002**, *16*, 592.
(2) Salmans, M. L.; Zhao, F.; Andersen, B. *Breast Cancer Res.* **2013**, *15*, 204.
(3) Zhou, W.; Pan, H.; Xia, T.; Xue, J.; Cheng, L.; Fan, P.; Zhang, Y.; Zhu, W.; Xue, Y.; Liu, X.; Ding, Q.; Liu, Y.; Wang, S. *J. Biomed. Sci.* **2014**, *21*, 97.
(4) Walker, L. C.; Harris, G. C.; Holloway, A. J.; McKenzie, G. W.; Wells, J. E.; Robinson, B. A.; Morris, C. M. *Cancer Genet. Cytogenet.* **2007**, *178*, 94.
(5) Tiago, D. M.; Conceição, N.; Caiado, H.; Laizé, V.; Cancela, M. L. *FEBS Lett.* **2016**, *590*, 1234.
(6) Tanaka, M.; Ichikawa-Tomikawa, N.; Shishito, N.; Nishiura, K.; Miura, T.; Hozumi, A.; Chiba, H.; Yoshida, S.; Ohtake, T.; Sugino, T. *BMC Cancer* **2015**, *15*, 53.
(7) Walia, V.; Yu, Y.; Cao, D.; Sun, M.; McLean, J. R.; Hollier, B. G.; Cheng, J.; Mani, S. A.; Rao, K.; Premkumar, L.; Elble, R. C. *Oncogene* **2012**, *31*, 2237.
(8) Huang, C.-Y.; Zhao, J.-J.; Lv, L.; Chen, Y.-B.; Li, Y.-F.; Jiang, S.-S.; Wang, W.; Pan, K.; Zheng, Y.; Zhao, B.-W.; Wang, D.-D.; Chen, Y.-M.; Yang, L.; Zhou, Z.-W.; Xia, J.-C. *PloS One* **2013**, *8*, e69155.
(9) Shi, C.-X.; Long, M. A.; Liu, L.; Graham, F. L.; Gauldie, J.; Hitt, M. M. *Mol. Ther.* **2004**, *10*, 758.
(10) J, O.; V, B.; J, P.; P, F.; P, D.; B, V.; R, H. *OncoTargets Ther.* **2015**, *8*, 1523.
(11) Herrmann, P.; Aronica, S. M. *SpringerPlus* **2015**, *4*, 245.
(12) Pandey, V.; Wu, Z.-S.; Zhang, M.; Li, R.; Zhang, J.; Zhu, T.; Lobie, P. E. *Breast Cancer Res.* **2014**, *16*, 429.
(13) Huang, Y.-K.; Fan, X.-G.; Qiu, F. *Int. J. Mol. Sci.* **2016**, *17*, 661.
(14) Yang, G.-D.; Yang, X.-M.; Lu, H.; Ren, Y.; Ma, M.-Z.; Zhu, L.-Y.; Wang, J.-H.; Song, W.-W.; Zhang, W.-M.; Zhang, R.; Zhang, Z.-G. *Int. J. Clin. Exp. Patho.* **2014**, *7*, 1348.
(15) Li, S.; Xie, Y.; Zhang, W.; Gao, J.; Wang, M.; Zheng, G.; Yin, X.; Xia, H.; Tao, X. *J. Surg. Res.* **2015**, *193*, 255.
(16) Sloan, E. K.; Stanley, K. L.; Anderson, R. L. *Oncogene* **2004**, *23*, 7893.
(17) Klein, R. M.; Bernstein, D.; Higgins, S. P.; Higgins, C. E.; Higgins, P. J. *Exp. Dermatol.* **2012**, *21*, 551.
(18) Forget, M. A.; Turcotte, S.; Beauseigle, D.; Godin-Ethier, J.; Pelletier, S.; Martin, J.; Tanguay, S.; Lapointe, R. *Brit. J. Cancer* **2007**, *96*, 646.
(19) Acton, S. L.; Scherer, P. E.; Lodish, H. F.; Krieger, M. *J. Biol. Chem.* **1994**, *269*, 21003.
(20) Toh, B.-H.; Kyaw, T.; Tipping, P.; Bobik, A. *Cell. Mol. Immunol.* **2013**, *10*, 379.
(21) Woodfin, A.; Voisin, M.-B.; Nourshargh, S. *Atertio. Thromb. Vasc. Biol.* **2007**, *27*, 2514.
(22) Jamieson, T.; Clarke, M.; Steele, C. W.; Samuel, M. S.; Neumann, J.; Jung, A.; Huels, D.; Olson, M. F.; Das, S.; Nibbs, R. J. B.; Sansom, O. J. *J. Clin. Invest.* **2012**, *122*, 3127.
(23) Corella, D.; Ordovás, J. M. *Ageing Res. Rev.* **2014**, *18*, 53.
(24) Cenciarelli, C.; Hou, D.; Hsu, K.; Rellahan, B.; Wiest, D.; Smith, H.; Fried, V.; Weissman, A. *Science* **1992**, *257*, 795.